Northumbria
University
NEWCASTLE

Integration of Tool Error Identification and Machining Accuracy Prediction into Machining Compensation in Flank Milling

Hangzhuo Yu[1], Shengfeng Qin[2], Guofu Ding[1], Lei Jiang[1], Lei Han[1]

[1]Institute of Advanced Design and Manufacturing, School of Mechanical Engineering, Southwest Jiaotong University, Chengdu, China

[2]School of Design, Northumbria University, Newcastle upon Tyne, UK

Corresponding author:

Lei Jiang, Institute of Advanced Design and Manufacturing, School of Mechanical Engineering, Southwest Jiaotong University, Chengdu, 610031, China

Email: jianglei0506@163.com

Abstract: In a flank milling process, the tool rotation profile error induced by its radial dimension error, setup error, tool deflection and wear has a great influence on the dimensional accuracy of the machined components. In this paper, we present an integrated identification of tool error, prediction of machining accuracy and compensation methodology for tool profile error to improve the machining accuracy. Firstly, the tool errors are divided into static and dynamic errors based on the error characteristics and the corresponding error identification methods are established to recognize the tool error parameters. Secondly, the machining accuracy is predicted by a prediction model, and the tool error parameters are input into this model. Thirdly, a new tool error compensation method is developed and incorporated in the corresponding NC codes. Finally, some machining experiments have been carried out to validate the proposed identification-prediction-compensation methodology, and the results show that this methodology is effective.

Keywords: Tool Rotation Profile Error, Error Identification, Accuracy Prediction, Error Compensation, Flank Milling

1. Introduction

In a flank milling process, the entire effective length of a tool is in contact with the

workpiece and the side of the milling tool is utilized as the primary cutting surface, the machined surface can be described as simply a line moving in space[1]. There are many factors affect the machining accuracy such as tool path errors[2,3] caused by the geometric errors, thermal errors of machine tool and tool rotation profile error caused by tool run-out error[4], tool deflection[5] and tool wear[6] especially for a difficult-to-cut material. The machining error due to machine tool inaccuracy can be easily identified and compensated by the ISO standards as the geometric errors of machine tool are static errors[3,7]. However, it is difficult to accurately deal with tool rotation profile error because some tool errors such as tool deflection and wear are dynamic changes in milling process.

Many researchers have devoted to modeling, identification and compensation for various tool errors, which are crucial to improve the machined quality and precision. For the tool dimension error and setup error, Arizmendi[8] and Artetxe[9] considered the tool parallel axis offset and setting error so that the tool axis tilt between the tool and the spindle axis lead to run-out errors are dealt with. So Arizmendi and Krüger[10] established surface topography prediction models for flank milling and considered the influence of tool run-out variables on the topography, these models successfully establish the mapping relationship between tool run-out and surface accuracy. But, in these models, input variable contains lots of run-out parameters such as tool parallel axis offset, tool axis tilt angle, tilt angular position and so on, how to identify these parameters correctly is critical for surface prediction. Many scholars presented identification methods based on the distribution of the average cutting force[11-13], they obtained the run-out parameters from process force through experiments. For the tool deflection, Yuan et.al[14] believe that cutting force can easily induce tool deflection thus make the tool center deviates the desired trajectory and causes dimension error. So Yuan and Zeroudi[15] established dimension error prediction models based on the tool deflection in ball-end milling, they considered the tool as a cantilever beam and the milling force as equivalent concentrated force imposed on the working point, and the deflection calculation method considered the Euler Bernoulli cantilever beam equations. Larue[16] and Islam[5] et.al established prediction models considering the influence of

tool deflection on flatness defects in flank milling, in these models the correct force model was chosen and the tool deflection was calculated. Therefore, the determination of the tool run-out parameters and the calculation of tool deflection require the cutting force model. However, it is difficult to accurately evaluate the cutting force as it is comparatively nonlinear on industrial tool paths[17], and takes a lot of calculation time in an industrial context[15].

Tool wear is defined as the amount of loss of tool material on the contact surface between tool and workpiece, which directly leads to dimension error of workpiece and tool breakage[18]. Chinchanikar[19] and Liang[20] studied the influence of tool wear on machining surface, and pointed out the major challenges of these approaches are: measurement, modeling and simulation. For tool wear measurement methods, it can be divided into two types, direct and indirect measurement. Direct wear measurements are made using a microscope to measure tool wear at the edge of the worn tool[21], indirect wear measurements are made using sensors to monitor acoustic emissions, motor spindle speed, power consumption and force applied to the tool by workpiece[22,23]. However, direct measurements are complex or time-consuming and requires the stoppage of the machine tool to measure tool wear. Thus, Zhang[24] proposed a new approach based on shape mapping to acquire tool wear for ball end milling tool, the method does not require the stoppage of machine tool, then established an off-line tool wear prediction model[18] for assessing the degree of wear. For tool wear modeling, the process parameters, cutting time, and wear position constitute the input factors and tool wear is the output parameter for the model. Palanisamy[25] and Saini[26] developed models using regression and response surface methodology (RSM) techniques respectively with variable process parameters. However, these methods have defects of accuracy, in order to improve the prediction accuracy, Salimiasl[27] developed model using artificial neural network(ANN) techniques. Zhang[28] established tool wear estimation models using the least squares support vector machines(LS-SVM) and Kalman filter(KF) techniques respectively with variable process parameters, cutting time, and wear position. So, these methods such as ANN and SVM are more mature and have better prediction effect. For estimation of the effect

of tool wear on machining quality, Zhang[6] presented a surface topography model and an on-line simulation method of surface topography considering tool wear based on the tool wear identification[24] and modeling[18], this method can effectively evaluate the effect of tool wear on ball-end milling operation.

Other authors proposed some compensation methods specifically for tool deflection, Smaoui[29] and Biermann[30] developed compensation methods based on mirror correction to compensate tool deflection error, the methods modified the NC programs and required no reconstruction in CAM systems. Based on these results, Zeroudi[15] and Ma[31] et.al proposed compensation methods to compensate tool deflection error in five-axis ball-end milling by modifying tool tip and tool axis orientation, these methods are carried out by iterative operations, until the error is lower than prescribed tolerance criterion. However, there is lack of effective compensation analysis for the other tool errors.

In some machining situation especially for difficult-to-cut material in flank milling, the tool radial dimension error, setup error, tool deflection and wear are always happening at the same time. However, few people simultaneously consider these four kinds of tool errors to predict machining accuracy and compensate errors. The tool wear will lead to a reduction in the tool radius and the increase of the cutting force, thus affecting the tool deflection, which will in return affect the tool wear[32]. Therefore, tool wear and tool deflection have coupling effects, it is difficult to describe this approach accurately in a mathematical way, and some numerical approach is difficult to use in an industrial context as the complexity of data programming[15].

In this paper, an identification-prediction-compensation methodology that contains the four kinds of tool errors is presented in a flank milling process. First of all, an identification method based on cutting experiments is proposed to recognize the tool error parameters. Then a new prediction model based on a pre-existing prediction model[33] is established to predict the machining accuracy, in which the tool error parameters are taken into account. At last, the tool error is compensated using a compensation method by correcting the NC codes. The identification method is based on the cutting experiments, so this method does not require complex theoretical

calculation. These four kinds of tool errors can be considered simultaneously in the prediction of machining accuracy and tool error compensation, so the prediction accuracy and machined quality can be improved.

The structure of this paper is as follows. Section 2 analyses the methodological and tool errors. Section 3 introduces the identification method for tool static error and dynamic error. Section 4 introduces the prediction model for machining accuracy. Section 5 describes the compensation method for tool errors. Section 6 evaluates the methods with some machining experiment tests. Finally, the conclusions are drawn in section 7.

2. Methodological and tool error analysis

The operation of the above three steps is as follows: First, for the identification of tool error parameters, we can directly (1) measure the tool static error parameters before machining, (2) obtain the dynamic error values by trial cutting in various machining situations using the identification method, and (3) set up an error database to further establish a dynamic error estimation model to calculate the predicted values in subsequent processing. Second, import the tool error predicted values into the prediction model of machining accuracy to realize the accuracy prediction. Finally, based on the above work, an error compensation method is established by modifying tool tip position based on mirror correction and iterative principle.

Tool error analysis

The radial dimension error, setup error, tool deflection and wear are the main factors to affect the tool rotation profile error, thus affect the shape of tool-workpiece contact line as shown in Fig. 1.

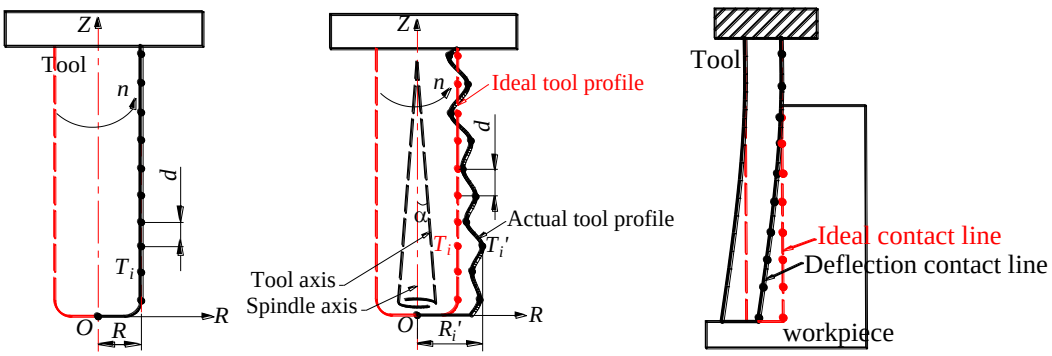

(a) Ideal rotation profile

(b) Actual rotation profile with dimension error and setup error

(c) Illustration of tool deflection

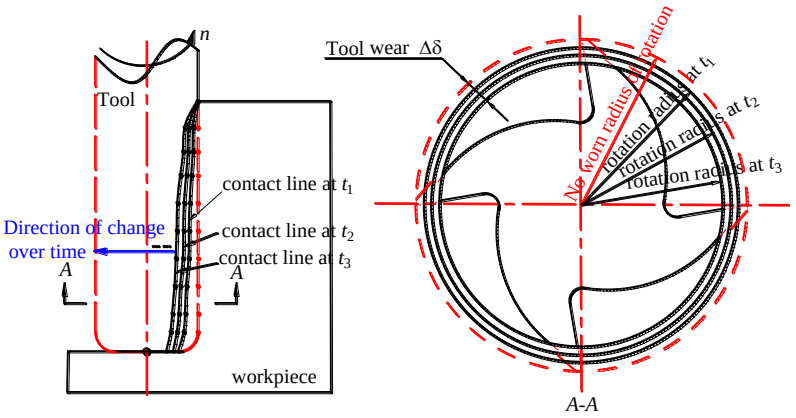

(d) Illustration of tool wear

Fig. 1 Illustration of tool errors

The ideal envelope formed by tool rotation should be a cylinder with a radius R, as shown in Fig. 1 (a). The tool dimension error is generated in tool manufacturing or grinding process, the tool setup error caused by misalignment of the tool rotation axis and the spindle rotation axis can result in a cone-shaped revolving body formed by tool axis with an angle α between the tool axis and the spindle axis. Therefore, the actual radius of section in actual tool revolving body along tool axis is constantly changing caused by the dimension error and setup error, as shown in Fig. 1 (b). Tool deflection leads to cutting edge far away from the ideal edge, so it is equivalent to the reduction of tool rotation radius, shown in Fig. 1 (c). Tool wear is defined as the change of tool shape from its original shape during machining process, which will also lead to a reduction in tool rotation radius, as shown in Fig. 1 (d).

For the above four kinds of tool errors, radial dimension error and setup error are constants that do not change with time and not affected by cutting condition, so these errors can be defined as static error. While tool deflection and wear are related to machining condition and change with cutting time, meanwhile, tool deflection and wear are equivalent to the dynamic reduction of tool rotation radius at different positions with time. So, we don't need to separate them in measurement rather than take these two kinds of errors as a synthesized-tool dynamic error, this dynamic error results in the reduction of the tool rotation radius whereby leading to undercut. Reference

to[4,5,6,8,32,34], the classification of tool errors as shown in Table 1.

Table 1 Tool errors classification

Tool errors		Influence factors	Change characteristics
Static error	Dimension error Setup error	Not affect by machining condition	Do not change with cutting time
Dynamic error	Tool wear	Tool-workpiece material property, tool geometry and machining parameters	Significant change with cutting time
	Tool deflection	Cutting force, tool geometry and machining parameters	Change with cutting time

3. Tool error parameters identification

There is a mapping relationship between the tool rotation radius and the normal machining error[14] in a plane machining, as shown in Fig. 2. Therefore, a new identification method based on shape mapping is proposed to obtain tool errors by cutting plane experiments. In the experiments, tool cuts straight along the X axis of the machine tool, other errors such as machine tool errors and control system errors have little influence, and only tool errors have great influence on the normal machining error. However, the normal machining error measured is the reflective result from the comprehensive tool errors including static and dynamic errors. It is necessary to separate the static and dynamic error parameters in order to establish the dynamic error estimation model. Therefore, firstly, we can directly measure the static error before machining, and then deduce the influence of static error on the normal machining error of measurement, so as to get the dynamic error parameters.

3.1. Static error parameters identification with direct measurement on tool

Tool errors lead to the rotation radius change along tool axis, as shown in Fig. 1. A radius measuring coordinate system *ROZ* is established, discretizing the cutting edges in the *Z* direction, so a series of measuring points T_i' (i=1,2⋯⋯,m) are selected to measure the tool rotation radius and the corresponding radius are R_i'. The distance between two adjacent measuring points is d, where m=int(L_T/d), and L_T is the effective length of cutting edge. The ideal radius for the ideal measuring points T_i is R. So the

tool radius R_i' only considering the influence of tool static error can be expressed as:

$$R_i' = \Delta R_i + R \quad (1)$$

Where ΔR_i represents the tool rotation radius error at T_i', if $R_i' > R$, then $\Delta R_i > 0$; else $\Delta R_i < 0$.

Reference[33] pointed out that the radius R_i' can be measured by laser tool measuring system, when measuring, the tool is mounted on the spindle and rotates with it, then tool moves downward along Z axis with a distance of *d*, a few seconds to stay and the rotation radius can be measured.

3.2. Dynamic error parameters identification with indirect measurement on machined surface

There is a mapping relationship between the dynamic error and the normal machining error in a plane machining especially using difficult-to-cut materials, as shown in Fig. 2. Therefore, the tool dynamic error can be indirectly identified by measuring the normal machining error on machined surface.

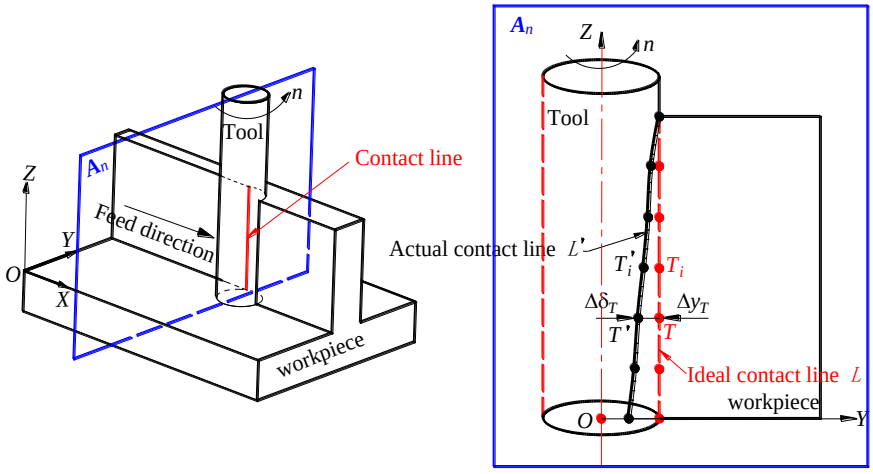

Fig. 2 Mapping relationship between the dynamic error and the normal machining error

A normal plane A_n perpendicular to the tool feed direction (X direction) is defined at a certain time t in machining process, thus the normal machining error can reflect the tool dynamic error in A_n.

In A_n, point T_i on ideal contact line L and the corresponding point T_i' on actual contact

line L' are selected as to explain the identification process. As tool dynamic error changes with cutting time, $\Delta\delta_i(t)$ refers to the tool dynamic error at time t corresponding to T_i', $\Delta y_i(t)$ refers to the normal machining error along Y axis at T_i' which can be measured by the coordinate measuring machine (CMM), ΔR_i refers to tool static error which is a constant had been obtained, thus the dynamic error $\Delta\delta_i(t)$ can be obtained by Eq.(2):

$$\Delta\delta_i(t) = \Delta R_i - \Delta y_i(t) \qquad (2)$$

The determination of time variables is very important, the tool moves keeping the fixed feed V_f, so the cutting time t_j (j=1,2,⋯⋯,k) corresponds to the cutting length L_j, and can be expressed as $t_j = L_j / V_f$. Therefore, the dynamic error at each cutting time can be obtained as long as the machining errors at each position is measured by CMM, as shown in Fig. 3.

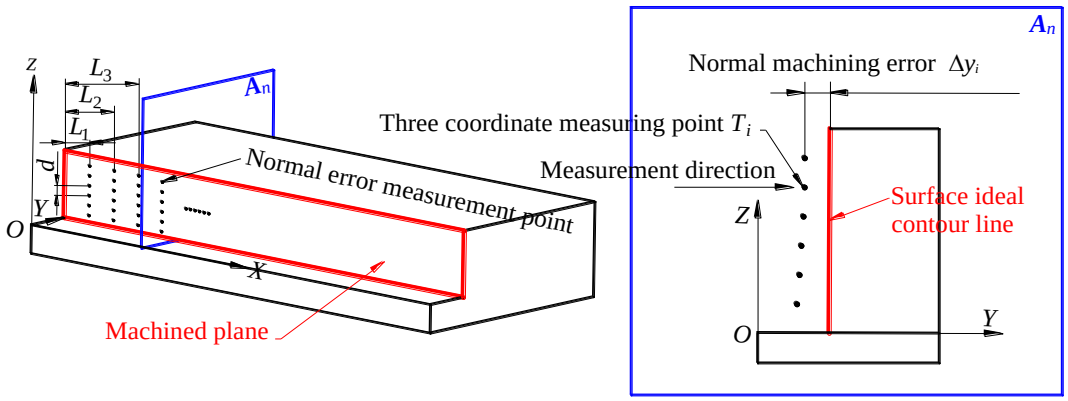

Fig. 3 Measurement of normal machining error for measuring points on machined Surface

In order to acquire the dynamic error at different axial positions of the tool, several measuring points are set along the cutting edge at each measuring place L_j. The distance between two adjacent measuring points is d, thus the height Z which is a distance calculated from the tool tip for each axial measuring point can be expressed as $Z=i \cdot d$.

Therefore, the dynamic error $\Delta\delta_i(t_j, Z)$ at T_i' can be expressed as:

$$\Delta\delta_i(t_j, Z) = \Delta R_i(i \cdot d) - \Delta y_i(L_j / V_f, i \cdot d) \qquad (3)$$

For the defined tool geometry and machining material, the tool dynamic error is affected by machining parameters (axial cutting depth a_p, feed rate V_f, spindle speed n

and radial cutting depth a_e). Therefore, we can set up an error database by trial cutting in various machining situations, and then establish an estimation model to calculate the predicted values in subsequent processing. The dynamic error estimation model is a non-linear relation model expressed as $\Delta\delta\left(a_p, n, V_f, a_e, t, Z\right)$, the input factors include a_p, V_f, n, a_e, cutting time t and cutting edge position Z, dynamic error $\Delta\delta$ is an output factor. In order to better express the nonlinear relation of input and output variables, the GA-BP neural network algorithm[35] is used to establish the estimation model.

The three-layer BP neural network is used in network training, the input layer of BP contains 6 neurons (represent a_p, V_f, n, a_e, t, Z), output layer contains 1 neuron (represents $\Delta\delta$), the linear transfer function is used as the transfer function of input and output layers, the hidden layer contains 4 neurons, the sigmoid tangent function is used as the transfer function of hidden layer, as shown in Fig. 4. The learning ratio is set as 0.05, and the performance error is set as 0.0001. The connection initial weights and thresholds of BP can be optimized by Genetic Algorithm (GA), as shown in Fig. 5.

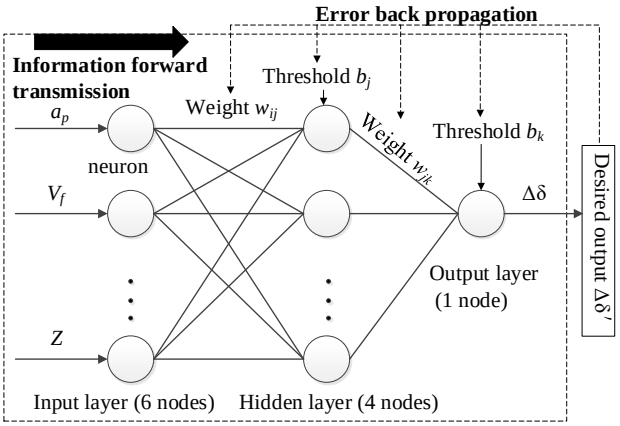

Fig. 4 The structure of BP neural network

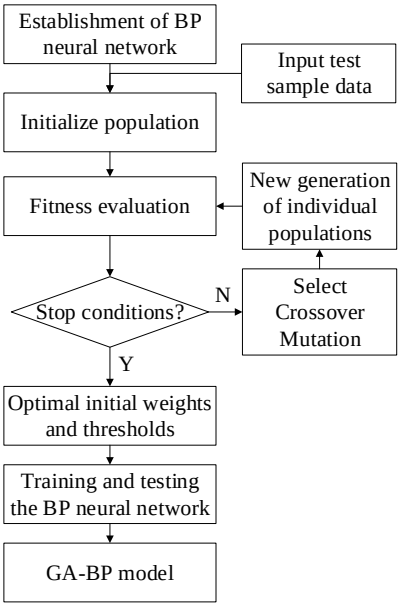

Fig. 5 The flow chart of GA-BP model

The population scale of GA is set as 50, the evolutional generation is set as 100, the crossover probability is set as 0.5, the mutation probability is set as 0.01, the fitness function $f(x) = \sum|\Delta\delta - \Delta\delta'|$ ($\Delta\delta$ and $\Delta\delta'$ are the predicted and desired output).

In this paper, the orthogonal experiment method is used to obtain the dynamic error

under the various machining parameters, and the experiment results are used to train the GA-BP algorithm for establishing the dynamic error estimation model, Section 6.1 gives details.

4. Machining accuracy prediction

According to the identification results of the tool errors, the machining accuracy can be predicted. In the early work, we proposed a prediction model[33] considering the influence of geometric error of machine tool and workpiece locating error. The tool contact points between the tool profile and workpiece play predominant roles in generating the milled surfaces[36], and these points can be calculated by the pre-existing prediction model. On this basis, we continue to introduce the tool error parameters to establish a new prediction model.

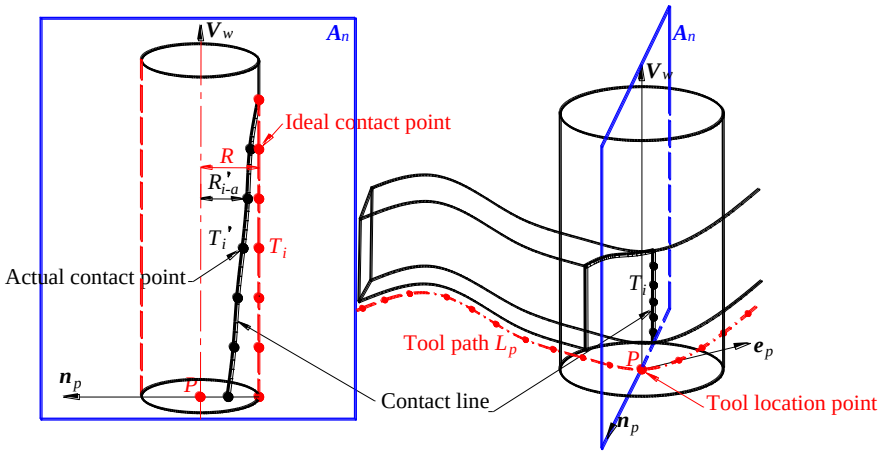

Fig. 6 Illustration of flank milling

As shown in Fig. 6, according to the pre-existing model, the actual tool location $\boldsymbol{P}' = \left(p_x', p_y', p_z'\right)^{\mathrm{T}}$, tool orientation $\boldsymbol{V}_w' = \left(v_x', v_y', v_z'\right)^{\mathrm{T}}$, normal unit vector $\boldsymbol{n}_p' = \left(n_{px}', n_{py}', n_{pz}'\right)^{\mathrm{T}}$, and tangent vector $\boldsymbol{e}_p' = \left(e_{px}', e_{py}', e_{pz}'\right)^{\mathrm{T}}$ in workpiece coordinate system corresponding to the actual tool location point P' in the CL-File can be calculated considering the influence of tool path errors. On this basis, we established a new model to calculate a serious of tool contact points T_i' for P' through input the tool static and dynamic error parameters.

As shown in Fig. 1 and Fig. 2, the rotation radius corresponding to each tool contact point will deviate from the ideal value as the effect of tool errors, which will lead to the

tool contact points on the contact lines deviate from the ideal position. When cutting hard materials, both the static and dynamic errors have an effect on the tool rotation radius. Although the static error is fixed while the dynamic error varies with time, but the influence from both is independent, thus their influence can be superimposed. Therefore, the rotation radius R'_{i_a} corresponding to T'_i can be expressed by Eq.(4):

$$R'_{i\_a} = R'_i - \Delta\delta_i\left(a_p, n, V_f, a_e, t, Z\right) \quad (4)$$

Where R'_i represents the radius affected by static error, $\Delta\delta$ represents the dynamic error values calculated by GA-BP estimation model.

In actual machining process, the machining parameters a_p, V_f, n, a_e are generally fixed in a whole or local machining area, so dynamic error in a certain cutting height Z varies with time t, it is critical to introduce the cutting time t to the estimation model correctly. The cutting time t_p corresponding to tool location point P can be determined by the tool trajectory (NC code). Assuming that the tool is processed from the starting point P_0 with a fixed feed rate V_f, thus the time t_p can be expressed as:

$$t_p = \left(P_0P_1 + P_1P_2 + \mathrm{L} + P_{i-1}P\right)/V_f \quad (5)$$

Where P_iP_j represents the distance from point P_i to point P_j, the coordinates of P_i and feed rate V_f can be obtained from the NC code.

Therefore, the 6 input factors to the GA-BP estimation model can be acquired, and the dynamic error $\Delta\delta_i$ at T'_i can be calculated, Fig. 7 gives the detail.

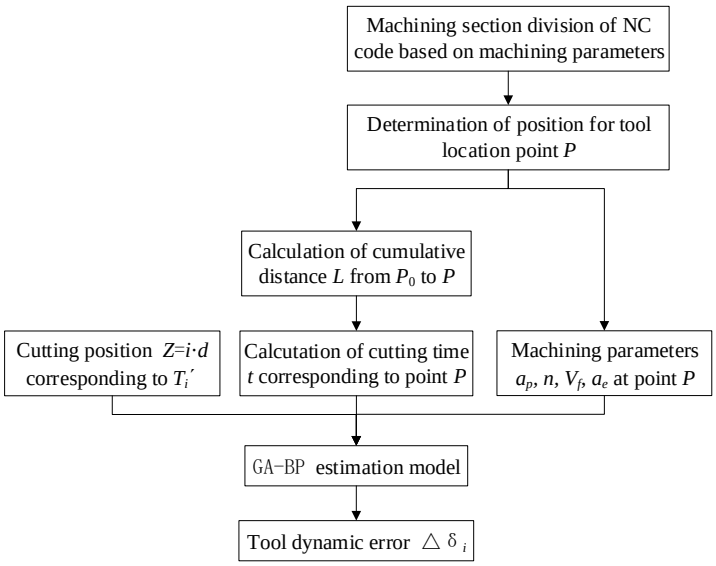

Fig. 7 Calculation flow of tool dynamic error for tool contact points in machining process

The coordinates of actual tool contact points T_i' corresponding to P' can be calculated by Eq.(6):

$$\boldsymbol{T}_i' = \begin{pmatrix} T_{ix}' \\ T_{iy}' \\ T_{iz}' \end{pmatrix} = \begin{pmatrix} p_x' - R_{i\_a}' \cdot n_{px}' + Z \cdot v_x' \\ p_y' - R_{i\_a}' \cdot n_{py}' + Z \cdot v_y' \\ p_z' - R_{i\_a}' \cdot n_{pz}' + Z \cdot v_z' \end{pmatrix} \tag{6}$$

According to the above calculation process, a series of tool contact points corresponding to each tool location point can be calculated. At last, the tool contact points on the finial machined surface can be obtained by the prediction method, then the normal machining error also can be calculated according to these points[15], which providing a reference for tool errors compensation.

5. Tool errors compensation

According to the results of identification and machining accuracy prediction, tool errors can be compensated. Usually, the influence of tool dynamic error is greater than static error when machining hard materials. Therefore, the tool error is equivalent to the reduction of the tool radius, thus leads to undercut, so the compensation of tool error is adjusting the position of tool in the normal direction so as to correct the rotation radius thus reduce the machining error. Compensation is implemented by modifying the NC code, but the adjustment of the tool tip does not involve the adjustment of the tool axis orientation. However, the tool error is highly nonlinear change in the direction of axial depth, so three compensation methods are assumed, as shown in Fig. 8.

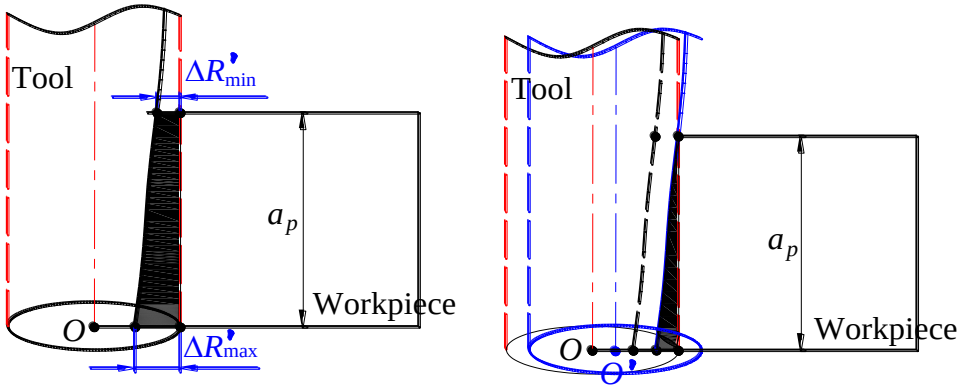

(a) Uncompensated (b) Compensated for $\Delta R'_{\min}$

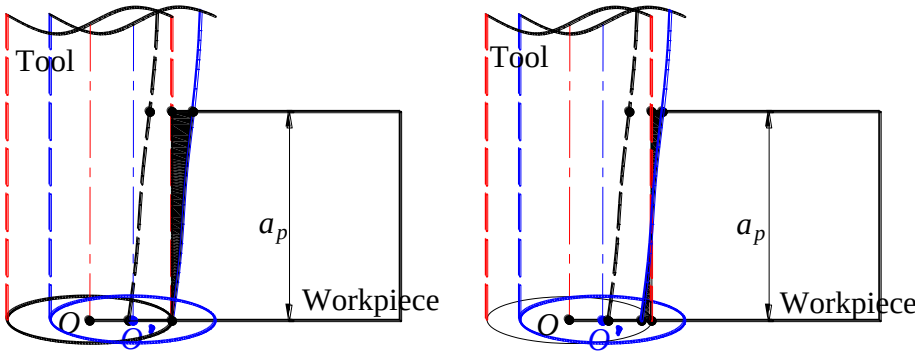

(c) Compensated for $\Delta R'_{\max}$ (d) Compensated for $\Delta\bar{R}'$

Fig. 8 Referenced tool position

The tool rotation radius error $\Delta R'_i$ can be expressed as $\Delta R'_i = R'_{i\_a} - R$. Fig. 8(a) shows an uncompensated milled workpiece. Fig. 8(b) represents the case when $\Delta R'_{\min}$ is chosen as the compensation reference. Fig. 8(c) represents the case when $\Delta R'_{\max}$ is chosen as the compensation reference. Fig. 8(d) represents the case when the average value $\Delta\bar{R}' = \frac{1}{n}\sum_{i=1}^{n}\Delta R'_i$ is chosen as the compensation reference. It can be observed that workpiece after compensation has varying amount of "under-cut" and "over-cut" for all cases. In order to reduce the influence of tool errors, $\Delta\bar{R}'$ is chosen as the compensation reference in this work. Therefore, the offset distance along normal direction for tool is $\Delta\bar{R}'$, as shown in Fig. 9.

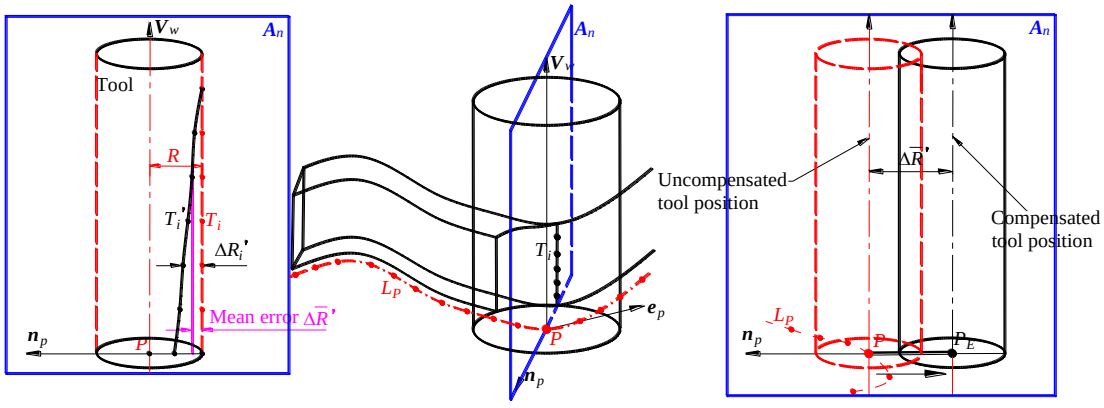

Fig. 9 Illustration of tool error compensation

However, the offset distance is not equal to the prediction error, because the change of the tool position will change the radial cutting depth a_e, and finally a new tool error value will be formed. It is necessary to carry out iterative operation, until the machining

error is lower than prescribed tolerance criterion for the machined surface. Take the location point P on L_p as an example, assume the coordinates of P is $\boldsymbol{P}_w$=（p_x，p_y，p_z）$^{\mathrm{T}}$, the overall procedures of tool path modification are shown in Fig. 9 and summarized as follows:

(1) The nominal strategy has to be programmed in CAM software to generate the CL-File.

(2) This file is treated by the accuracy prediction model, and the tool dynamic error evolution is obtained all along the tool trajectory, so the radius error $\Delta R'_{i\_1}$ corresponding to tool contact points T_i' for P can be calculated.

(3) The mean error $\Delta\bar{R}'_1 = \dfrac{1}{n}\sum_{i=1}^{n}\Delta R'_{i\_1}$ is obtained.

(4) Offset the tool to a distance $\Delta\bar{R}'_1$ in the opposite direction of the normal vector $\boldsymbol{n}_p = \left(n_{px}, n_{py}, n_{pz}\right)^{\mathrm{T}}$,thus point P move to P_E, and PP_E= $\Delta\bar{R}'_1$. Therefore, the coordinates of the compensated tool location point P_E can be calculated by Eq.(7).

$$\boldsymbol{P}_E = \begin{pmatrix} P_{Ex} \\ P_{Ey} \\ P_{Ez} \end{pmatrix} = \begin{pmatrix} p_x - \Delta\bar{R}'_1 \cdot n_{px} \\ p_y - \Delta\bar{R}'_1 \cdot n_{py} \\ p_z - \Delta\bar{R}'_1 \cdot n_{pz} \end{pmatrix} \quad (7)$$

(5) The radial cutting depth a_e becomes a_e+PP_E after the tool moves, replacing the adjusted machining parameters into the dynamic error estimation model to calculate the new error $\Delta R'_{i\_2}$ and the machining error can be calculated by prediction model.

(6) If the machining error is lower than prescribed tolerance criterion, the compensated tool position is determined. Otherwise, the process returns to step (3), repeating the procedure iteratively till tolerance criterion is satisfied.

According to the above process, the tool errors compensation can be realized by adjusting tool position for each tool location point.

In summary, the flow of identification-prediction-compensation methods for tool errors is shown in Fig. 10.

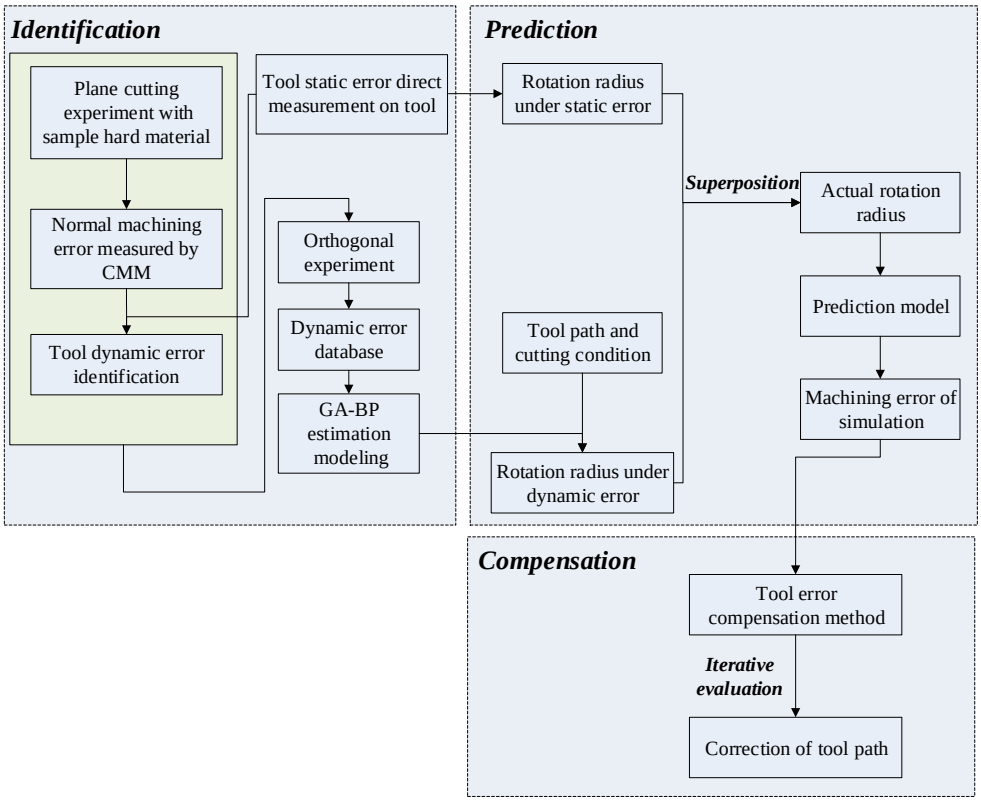

Fig. 10 Flow chart of the identification-prediction-compensation methods

6. Experimental validation

6.1. Experiment for tool error parameters identification

The identification method can be validated by carrying out a series of plane milling experiments, and a single factor experiment and an orthogonal experiment are set up.

(1) Single factor experiment

The plane machining experiment were performed on a machine center DMG-60, the cutting conditions are shown in Table 2, the cutting tool shown in Fig. 11.

Table 2 Cutting conditions for experiments

Tool	Ø16*40*92*16 high speed steel
Workpiece material	Stainless steel
Blank size	255 mm× 255 mm× 20 mm
Machining parameters	a_p=14 mm, a_e=1 mm, V_f=27 mm/min, n=270 r/min
Machining mode	Plane machining

Fig. 11 Cutting tool for experiments

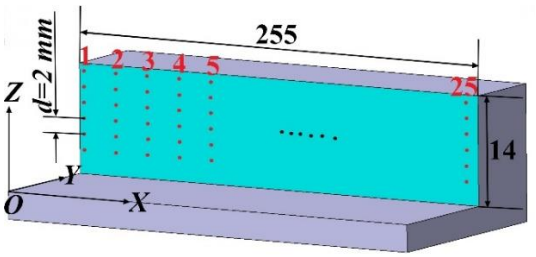

Fig. 12 The distribution of measuring points on machined plane

Static error measurement

After installation, the tool rotates with the spindle, the distance between two adjacent measuring points is d=2 mm, then the rotation radius corresponding to 6 measuring points was measured by a Renishaw laser tool measuring system (model NC4). Therefore, the static errors corresponding to these measuring points as shown in Table 3.

Table 3 Measurement results of tool static error unit: mm

Measuring point i （direction along the tool tip to hilt）	Z	Direct measurement radius	Tool static error ΔR_i
1	3	8.024	0.024
2	5	8.021	0.021
3	7	8.013	0.013
4	9	8.012	0.012
5	11	8.010	0.010
6	13	8.009	0.009

Dynamic error identification

A plane was machined use stainless steel, the normal machining error values of 150 points (6 lines*25 column) on the plane were measured by CMM, and the distance d=2 mm, as shown in Fig. 12. The measurement results of normal machining error are shown in Fig. 14, and the identification results of dynamic error are shown in Fig. 15.

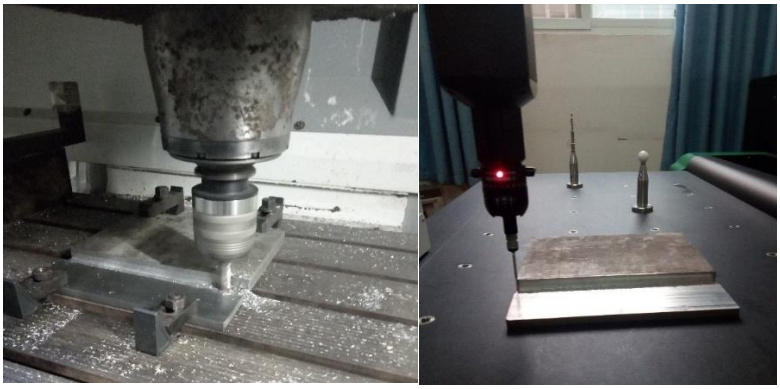

Fig. 13 Machining and measuring process of experiment

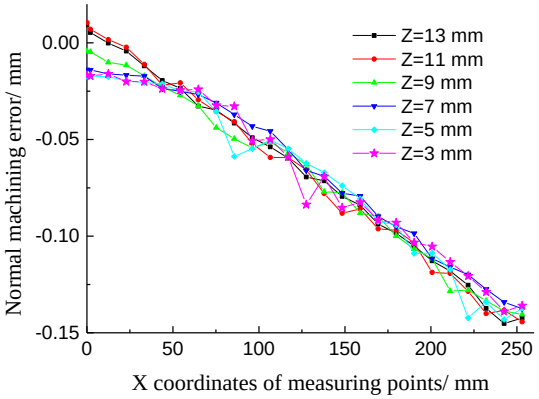

Fig. 14 Measurement results of machining error

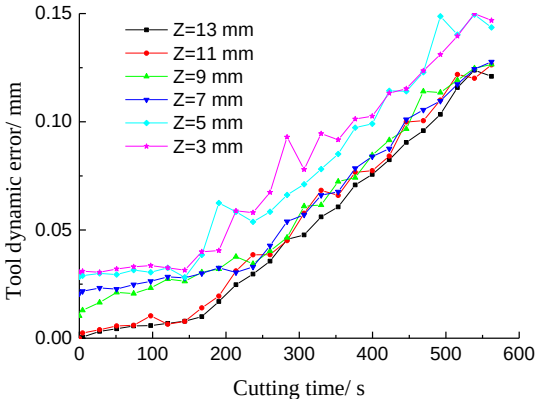

Fig. 15 Identification results of dynamic error

The shape change of contact line between the tool and the workpiece can be constructed by the dynamic error values for measuring points, as shown in Fig. 16.

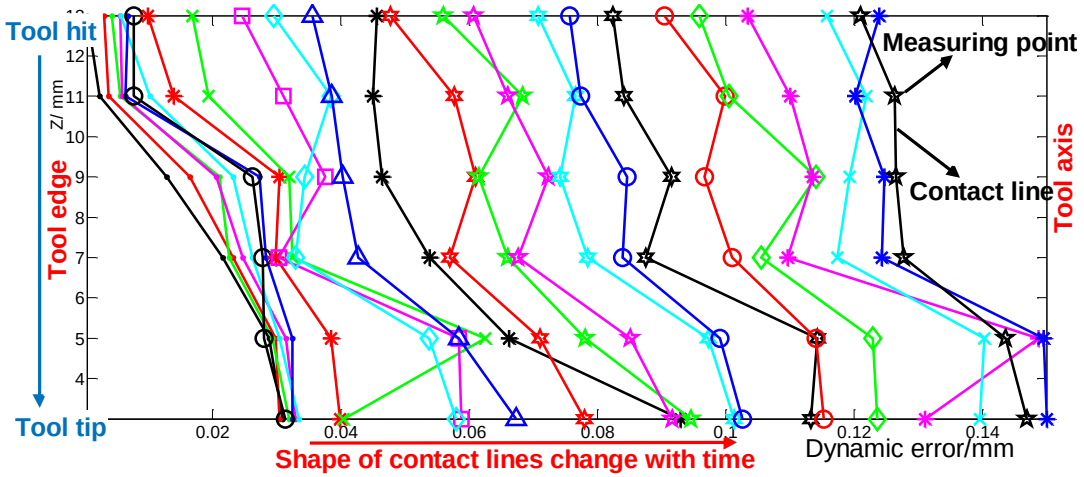

Fig. 16 Shape change of contact line in machining

From Fig. 15 and Fig. 16, we can see that the shape of contact line is constantly changing and approaching the tool axis as the dynamic error increases with time. Meanwhile, there is a phenomenon that the radius variation rate in different depth is different, and the greater the depth is, the greater the dynamic error. That is because the greater the depth is, the greater the cutting force, and the more serious the tool wear and deflection are.

(2) Multi-factor orthogonal experiment

In order to acquire the train data to establish the GA-BP estimation model $\Delta\delta\left(a_p, n, V_f, a_e, t, Z\right)$, the multi-factor orthogonal method is selected to design machining experiments, the orthogonal array $L_{16}(4^4)$ for variables a_p, V_f, n, a_e (variables

t and *Z* are reflected in measurement) has been used to construct 16 sets of experiments. The designed orthogonal experiment parameters are shown as Table 4.

Table 4 Orthogonal experiment parameters

Experiment number	a_p (mm)	n(rad/min)	V_f(mm/min)	a_e(mm)
1	10	2900	600	1
2	10	3200	800	1.3
3	10	3500	1000	1.6
4	10	3800	1200	1.9
5	13	2900	800	1.6
6	13	3200	600	1.9
7	13	3500	1200	1
8	13	3800	1000	1.3
9	16	2900	1000	1.9
10	16	3200	1200	1.6
11	16	3500	600	1.3
12	16	3800	800	1
13	19	2900	1200	1.3
14	19	3200	1000	1
15	19	3500	800	1.9
16	19	3800	600	1.6

The dynamic error values in each experiment can be attained by the identification method and then the dynamic error GA-BP estimation model can be established according to these data. The prediction results of the GA-BP evaluation model are shown as shown in Fig. 17.

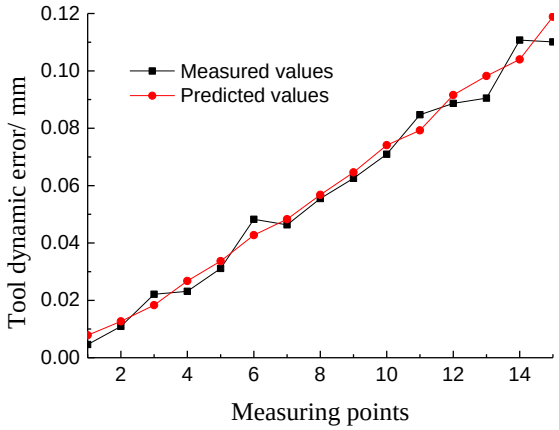

Fig. 17 Comparison of predicted values and measured values for GA-BP estimation model

From Fig. 17, the proposed GA-BP model can predict tool dynamic error with maximum error on an average of 4 μm compared with the actual tool error. Therefore, the GA-BP estimation model can be used to predict the tool dynamic error.

6.2. Experimental for prediction and compensation

In order to verify the effectiveness of the prediction and compensation method, a cutting test was conducted by cutting a workpiece like the letter S, as shown in Fig. 18. Stainless steel is selected as work material, the tool path and is shown in Fig. 19.

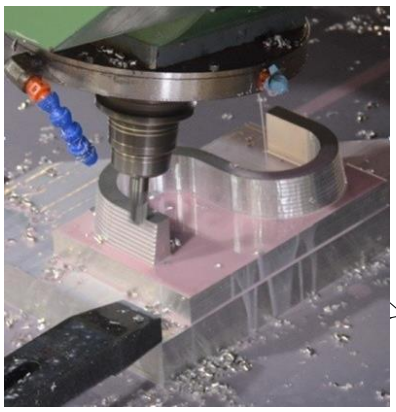

Fig. 18 The machined part

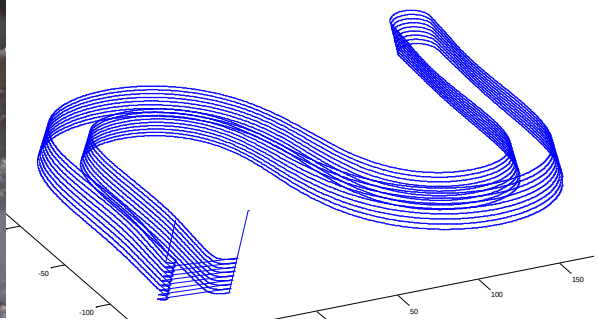

Fig. 19 Tool path of the experiment part

The distribution of ideal and actual tool contact points on the swept surface can be calculated respectively by the prediction model. Part of the tool contact points distributed is shown in Fig. 20.

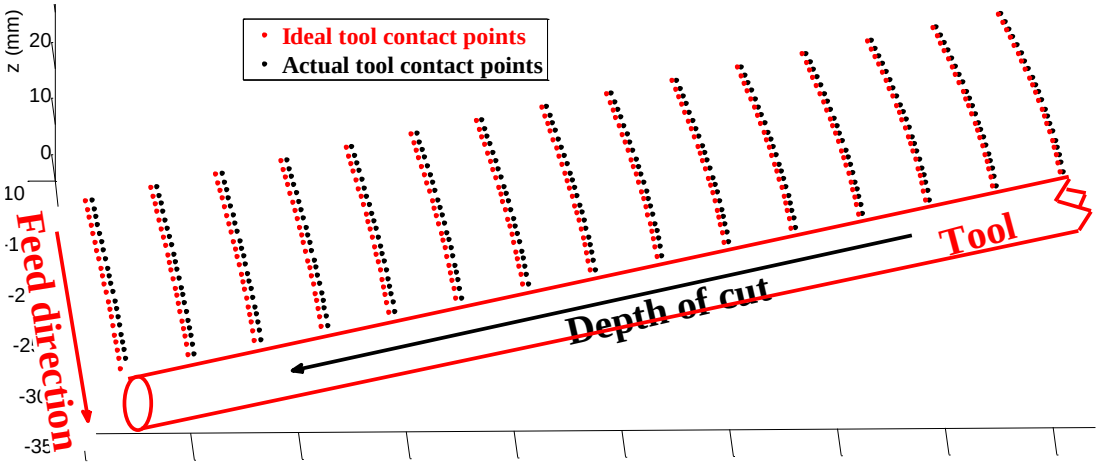

Fig. 20 The distribution of ideal and actual tool contact points on swept surface

According to the ideal and actual tool contact points, the normal machining error can be calculated to evaluate the accuracy of the machined surface[18]. The normal machining error of 15 points is shown in Fig. 21.

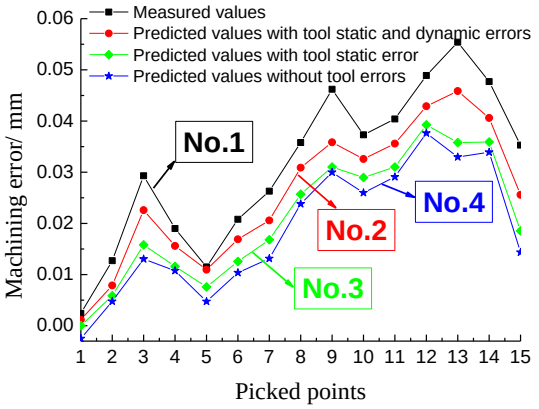

Fig. 21 Comparison of prediction and measured values for normal machining error

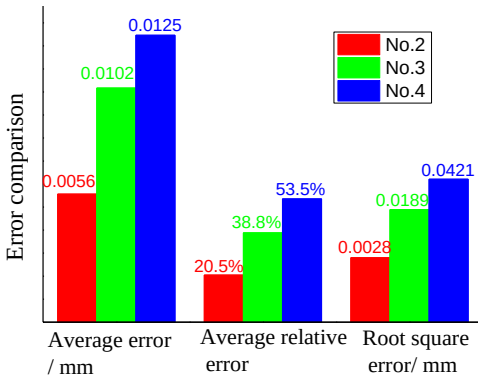

Fig. 22 Error comparison between the two groups of predicted values

In order to verify the effects of tool errors on machining accuracy, three groups of prediction results were calculated in the theoretical calculation. The first group is the prediction values calculated by the new model that considers tool static and dynamic errors (as No.2 curve shown in Fig. 21), the second group is the prediction values calculated by the new model that considers tool static error (as No.3 curve shown in Fig. 21), the third group is the prediction values that without considering the tool errors calculated by the pre-existing prediction model (as No.4 curve shown in Fig. 21). The normal machining error was measured by CMM on the machined surface (as No.1 curve shown in Fig. 21). The average errors, average relative errors and root mean square errors of the predicted values are shown in Fig. 22.

The pre-existing prediction model only considers the tool path errors caused by the geometric error of machine tool and workpiece locating error, while the new prediction model added the four kinds of tool errors based on the pre-existing model. Thus, the new model can simultaneously consider the influence of tool path error and the tool rotation profile error on surface machining accuracy. From Fig. 21 and Fig. 22, it is found that the values of No.2 are closest to No.1, and the average error, average relative error and mean square root error of predicted values in No.2 are less than No.3. It also found that the errors of No.3 are less than No.4, which indicates that the tool errors have certain influence on the machining accuracy; the new model has higher prediction accuracy by comparing with the prediction values of pre-existing model.

According to the iterative compensation method for tool errors, the position of each

tool location point was adjusted and the compensated NC code was acquired. The cutting test was carried out under two conditions: (1) without tool errors compensation and (2) with tool errors compensation. After machining, both machined parts were inspected for machining error by CMM. The comparative results are shown in Fig. 23.

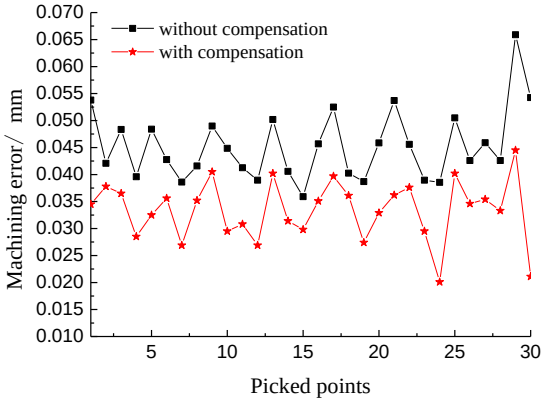

Fig. 23 The machining error of workpieces without/with compensation

Comparing the machining error measurement results of the two tested workpieces, it is found that machining accuracy has been improved about 35%~55%. Therefore, tool errors compensation method is effective.

7. Conclusions

This paper proposed an identification-prediction-compensation methodology for tool profile error caused by the tool radial dimension error, setup error, tool deflection and wear in flank milling process.

(1) Firstly, the tool profile error was divided into static error (radial dimension error and setup error) and dynamic error (tool deflection and wear) according to the characteristics of these errors. A new identification method for static and dynamic errors was established, the method was based on plane cutting experiments to recognize the tool error parameters, which does not require complex theoretical calculation. Then a tool dynamic error estimation model was established by the GA-BP neural network algorithm, which can describe the relationship between cutting situation and dynamic error, providing estimated error values for precision prediction.

(2) Secondly, a new prediction model considering the influence of tool errors was established based on a pre-existing prediction model, the static error parameters

and the dynamic error values acquired by GA-BP estimation model were introduced in the prediction model. Then the tool contact points along the tool trajectory were calculated to generate the machined surface, and the machining error were also calculated by these points. Some dedicated experimental tests have been carried out to verify the effectiveness of the identification and prediction methods.

(3) Finally, a compensation method was proposed to reduce the influence of tool errors, the method was based on the iterative evaluation and carried out by modifying the tool path. Then the effectiveness of the compensation method was verified through a comparative experiment.

8. Acknowledgement

This work is supported by the intelligent manufacturing found of the New Mode Application of Intelligent Manufacturing for the Key Components of High Speed Emu (2016ZNZZ01-05), from the ministry of industry and information technology, China.

9. References

[1] Sprott K, Ravani B. Cylindrical milling of ruled surfaces[J]. International Journal of Advanced Manufacturing Technology, 2008, 38(7-8):649-656.

[2] Zhu S W, Ding G F, Qin S F, et al. Integrated geometric error modeling, identification and compensation of CNC machine tools [J]. International Journal of Machine Tools & Manufacture, 2012, 52(1): 24-29.

[3] Miao E M, Liu H, Fan K C, et al. Analysis of CNC machining based on characteristics of thermal errors and optimal design of experimental programs during actual cutting process[J]. International Journal of Advanced Manufacturing Technology, 2016, 88(5):1-9.

[4] Arizmendi M, Fernández J, Gil A, et al. Effect of tool setting error on the topography of surfaces machined by peripheral milling[J]. International Journal of Machine Tools & Manufacture, 2009, 49(1):36-52.

[5] Islam M N, Han U L, Cho D W. Prediction and analysis of size tolerances achievable in peripheral end milling[J]. International Journal of Advanced

Manufacturing Technology, 2008, 39(1-2):129-141.

[6] Zhang C, Zhang H, Li Y, et al. Modeling and on-line simulation of surface topography considering tool wear in multi-axis milling process[J]. International Journal of Advanced Manufacturing Technology, 2015, 77(1-4):735-749.

[7] Eskandari S, Arezoo B, Abdullah A. Positional, geometrical, and thermal errors compensation by tool path modification using three methods of regression, neural networks, and fuzzy logic[J]. International Journal of Advanced Manufacturing Technology, 2013, 65(9-12):1635-1649.

[8] Arizmendi M, Fernández J, Gil A, et al. Effect of tool setting error on the topography of surfaces machined by peripheral milling[J]. International Journal of Machine Tools & Manufacture, 2009, 49(1):36-52.

[9] Artetxe E, Olvera D, Lacalle L N L D, et al. Solid subtraction model for the surface topography prediction in flank milling of thin-walled integral blade rotors (IBRs)[J]. International Journal of Advanced Manufacturing Technology, 2016:1-12.

[10] Krüger. M, Denkena. B. Model-based identification of tool runout in end milling and estimation of surface roughness from measured cutting forces[J]. International Journal of Advanced Manufacturing Technology, 2013, 65(5-8):1067-1080.

[11] Wan M, Zhang W H, Dang J W, et al. New procedures for calibration of instantaneous cutting force coefficients and cutter runout parameters in peripheral milling[J]. International Journal of Machine Tools & Manufacture, 2009, 49(14):1144-1151.

[12] Omar O E E K, El-Wardany T, Ng E, et al. An improved cutting force and surface topography prediction model in end milling[J]. International Journal of Machine Tools & Manufacture, 2007, 47(7–8):1263-1275.

[13] Yun W S, Cho D W. An improved method for the determination of 3D cutting force coefficients and runout parameters in end milling[J]. International Journal of Advanced Manufacturing Technology, 2000, 16(12):851-858.

[14] Yuan M, Wang X, Jiao L, et al. Prediction of dimension error based on the deflection of cutting tool in micro ball-end milling[J]. International Journal of

Advanced Manufacturing Technology, 2017(5):1-13.

[15] Zeroudi N, Fontaine M. Prediction of tool deflection and tool path compensation in ball-end milling[J]. Journal of Intelligent Manufacturing, 2015, 26(3):425-445.

[16] Larue A, Anselmetti B. Deviation of a machined surface in flank milling[J]. International Journal of Machine Tools & Manufacture, 2003, 43(2):129-138.

[17] Wang G, Li W L, Tong G, et al. Improving the machining accuracy of thin-walled parts by online measuring and allowance compensation[J]. International Journal of Advanced Manufacturing Technology, 2017(12–13):1-9.

[18] Zhang C, Zhou L. Modeling of tool wear for ball end milling cutter based on shape mapping[J]. International Journal on Interactive Design & Manufacturing, 2013, 7(3):171-181.

[19] Chinchanikar S, Choudhury S K. Predictive modeling for flank wear progression of coated carbide tool in turning hardened steel under practical machining conditions[J]. International Journal of Advanced Manufacturing Technology, 2015, 76(5-8):1185-1201.

[20] Liang X, Liu Z. Experimental investigations on effects of tool flank wear on surface integrity during orthogonal dry cutting of Ti-6Al-4V[J]. International Journal of Advanced Manufacturing Technology, 2017(12):1-10.

[21] Castejón M, Alegre E, Barreiro J, et al. On-line tool wear monitoring using geometric descriptors from digital images[J]. International Journal of Machine Tools & Manufacture, 2007, 47(12):1847-1853.

[22] Bhattacharyya P, Sengupta D, Mukhopadhyay S. Cutting force-based real-time estimation of tool wear in face milling using a combination of signal processing techniques[J]. Mechanical Systems & Signal Processing, 2007, 21(6):2665-2683.

[23] Chen J C, Chen J C. An artificial-neural-networks-based in-process tool wear prediction system in milling operations[J]. International Journal of Advanced Manufacturing Technology, 2005, 25(5-6):427-434.

[24] Zhang C, Liu X, Fang J, et al. A new tool wear estimation method based on shape mapping in the milling process[J]. International Journal of Advanced Manufacturing Technology, 2011, 53(1-4):121-130.

[25] Palanisamy P, Rajendran I, Shanmugasundaram S. Prediction of tool wear using regression and ANN models in end-milling operation[J]. International Journal of Advanced Manufacturing Technology, 2008, 37(1-2):29-41.

[26] Saini S, Sharma V S. Influence of cutting parameters on tool wear and surface roughness in hard turning of AISI H11 tool steel using ceramic tools[J]. International Journal of Precision Engineering & Manufacturing, 2012, 13(8):1295-1302.

[27] Salimiasl A, Ahmet Özdemir. Analyzing the performance of artificial neural network (ANN)-, fuzzy logic (FL)-, and least square (LS)-based models for online tool condition monitoring[J]. International Journal of Advanced Manufacturing Technology, 2016, 87(1-4):1-14.

[28] Zhang H, Zhang C, Zhang J, et al. Tool wear model based on least squares support vector machines and kalman filter[J]. Production Engineering, 2014, 8(1-2):101-109.

[29] Smaoui M, Bouaziz Z, Zghal A, et al. Simulation of the deflected cutting tool trajectory in complex surface milling[J]. International Journal of Advanced Manufacturing Technology, 2011, 56(5-8):463-474.

[30] Biermann D, Krebs E, Sacharow A, et al. Using NC-path deformation for compensating tool deflections in micromilling of hardened steel[J]. Procedia CIRP 1, 2012, 1(1):132-137.

[31] Ma W, He G, Zhu L, et al. Tool deflection error compensation in five-axis ball-end milling of sculptured surface[J]. International Journal of Advanced Manufacturing Technology, 2016, 84(5-8):1421-1430.

[32] Oliaei S N B, Karpat Y. Influence of tool wear on machining forces and tool deflections during micro milling[J]. International Journal of Advanced Manufacturing Technology, 2016, 84(9-12):1963-1980.

[33] Ding G F, Zhu S W, Yahya E, et al. Prediction of machining accuracy based on a geometric error model in five-axis peripheral milling process[J]. Proceedings of the Institution of Mechanical Engineers Part B Journal of Engineering Manufacture, 2014, 228(10):1226-1236.

[34] Slamani M, Chatelain J F, Hamedanianpour H. Comparison of two models for predicting tool wear and cutting force components during high speed trimming of CFRP[J]. International Journal of Material Forming, 2015, 8(2):305-316.

[35] Zhang J, Xu C, Yi M, et al. Design of nano-micro-composite ceramic tool and die material with back propagation neural network and genetic algorithm[J]. Journal of Materials Engineering & Performance, 2012, 21(4):463-470.

[36] Seo T I, Cho M W. Tool trajectory generation based on tool deflection effects in the flat-end milling process (II) —Prediction and compensation of milled surface errors—[J]. KSME International Journal, 1999, 13(12):918-930.

Appendix 1

Notation

R ideal radius of tool

ROZ radius measuring coordinate system

T_i' (i=1,2⋯⋯,n) actual tool contact points

R_i' series radius of tool rotation profile

T_i ideal tool contact points

d distance between the measuring points

m the number of measuring points

L_T the effective length of cutting edge

$\boldsymbol{A}_n$ normal plane

L ideal contact line

L' actual contact line

Δy the normal machining error

ΔR the tool rotation radius error

t cutting time

$\Delta\delta$ tool dynamic error

L_j machining length

V_f feed rate

Z cutting height

a_p axial cutting depth

n spindle speed

a_e radial cutting depth

P' actual tool location point

$\boldsymbol{V}_w'$ actual tool orientation in WCS

$\boldsymbol{n}_p'$ normal vector at P'

$\boldsymbol{e}_p'$ actual tangent vector

P ideal tool location point

α angle of between tool axis and spindle axis

$\boldsymbol{P}_w$ ideal tool location point in WCS